On the adjoint problem in duct acoustics and its solution by the Time Domain Wave Packet method

Fang Q. Hu,* Ibrahim Kocaogul[†]
Old Dominion University, Norfolk, Virginia, 23529

Xiaodong Li[‡]

Beijing University of Aeronautics and Astronautics, Beijing, 100083, China

The Time Domain Wave Packet (TDWP) method has the advantage of obtaining radiated sound by a given duct mode at all frequencies in one computation. It also makes possible the separation of the acoustic and shear flow instability waves. In this paper, the TDWP method will be applied to the adjoint duct acoustics problem. As a microphone records the sound radiated by all duct modes combined, the adjoint approach by TDWP method has the advantage of obtaining the relative mode strengths of all the propagating modes at all frequencies in one computation. The theoretical formulation of open duct adjoint problem and derivation of reciprocal relations are presented. The adjoint equations for the linearized Euler equations are formulated in the time domain for the Cartesian and cylindrical coordinates. The dispersion relations of the linear waves supported by the adjoint system are also discussed. It is shown that in a uniform mean flow, the dispersion relations for linear acoustic waves of the adjoint system are identical to that of the Euler equations under similar boundary conditions and the eigenfunctions (mode shapes) of the Euler and adjoint systems corresponding to different eigenvalues are orthogonal. These properties, particularly the orthogonality condition, lead to a reciprocal relation between the duct mode amplitudes and far field point sources in the presence of the exhaust shear flow. The adjoint equations are then solved numerically in reversed time by the TDWP method, in which a point source in the far field is enforced with a Broadband Acoustic Test Pulse time function. Application of the adjoint problem to NASA/GE Fan Noise Source Diagnostic Test (SDT) exhaust radiation problem is also presented.

I. Introduction

Recently, a Time Domain Wave Packet (TDWP) method has been developed for linear aeroacoustic computations. ¹³ It differs from the more conventional approach in that the modeling of the source time function is deliberately made to be a broadband temporal pulse. In the Time Domain Wave Packet method, the acoustic source is modeled as a wave packet by introducing a broadband and temporally compact time function. As the propagation properties of linear waves of all frequencies will be embedded in the propagation of the packet, the time domain simulation produces the results for all the frequencies within the numerical resolution. The numerical simulation needs to last only until the wave packet has exited the computational domain, making it more efficient than the conventional time domain approach where a time periodic state is required. In the TDWP method, solutions at all frequencies can be obtained by FFT of the time domain solution in a single time domain simulation.

^{*}Professor, Department of Mathematics and Statistics, AIAA associate fellow

[†]Graduate Student, Department of Mathematics and Statistics

[‡]Professor, School of Jet Propulsion, AIAA associate fellow

In this paper, the Time Domain Wave Packet (TDWP) method is applied to the open duct adjoint problem. The adjoint system for the linearized Euler equations with a general non-uniform mean flow is formulated in the time domain. There are many advantages afforded by the adjoint problem. In a forward radiation problem, usually the engine duct propagating modes are specified as the acoustic source inside the duct and far-field directivity of radiated sound is computed. In the adjoint problem, instead, a source can be placed at the far-field, representing the receiver/microphone, and the waves propagated into the duct from the far-field source is computed using the adjoint system. A reciprocity between the duct propagating mode and far-field sound is derived in the paper which produces the relative radiation strengths of all duct propagating (cut-on) modes to the particular microphone, after a modal decomposition of the waves inside the duct. This is potentially more efficient than computing the far field directivity from each duct mode separately when the number of observation points is smaller than the number of possible propagating duct modes. Combined with the Time Domain Wave Packet (TDWP) technique, relative strengths of all duct modes of all frequencies to the acoustic pressure at a particular far-field location can be determined in a single time domain computation. As a microphone records the radiated sound from all cut-on duct modes combined, solution of adjoint system can beneficial. Due to reciprocity, solutions of the adjoint problem can also serve to validate those of the forward problem.

Previously, adjoint systems for the linearized Navier-Stokes equations for incompressible flows have been studies (see for example [6,17,8] and the references cited within). Adjoint solutions have also been used in flow and noise controls.⁵ In [19], the adjoint equations for linearized Euler equations has been given in the frequency domain for an investigation of jet noise radiations. Point-to-point reciprocal relations were established in [19] for use in the prediction of jet noise. Reciprocal relation between duct radiating modes and the far-field sound was first studied in [1] without flow, in which case the governing equation for the acoustic pressure is self-adjoint. Reciprocal relations in acoustical fields in general flows have also been studied in [3,4,14,15] and many others, in particular in connection with the study in acoustics energy fields. However, as far we are aware of, the adjoint problem for open duct with flow in time domain has not been investigated in the literature.

The rest of the paper is organized as follows. In the next section, the adjoint system for the linearized Euler equations with a general mean flow is defined and formulated in the time domain. For convenience of its applications to duct acoustics, the adjoint system of equations for both the Cartesian and cylindrical coordinates are given. The special case of a uniform mean flow is considered in section 3. Orthogonality of eigenfunctions and some reciprocal relations are studied in section 4 and 5. Section 6 discusses issues related to the numerical implementation in solving the adjoint Green's function using the Time Domain Wave Packet method. Numerical results are presented in section 7 and concluding remarks are given in section 8.

II. Definition and formulation of adjoint systems

In this section, the adjoint system for the linearized Euler equations in the Cartesian and cylindrical coordinates will be discussed.

II.A. Cartesian Coordinates

Consider linearized Euler equations written in matrix form as

$$\frac{\partial \mathbf{w}}{\partial t} + \mathbf{A} \frac{\partial \mathbf{w}}{\partial x} + \mathbf{B} \frac{\partial \mathbf{w}}{\partial y} + \mathbf{C} \frac{\partial \mathbf{w}}{\partial z} + \mathbf{D} \mathbf{w} = 0 \tag{1}$$

where

$$\boldsymbol{w} = \begin{bmatrix} \rho' \\ u'_x \\ u'_y \\ u'_z \\ p' \end{bmatrix}, \quad \boldsymbol{A} = \begin{bmatrix} \bar{u}_x & \bar{\rho} & 0 & 0 & 0 & 0 \\ 0 & \bar{u}_x & 0 & 0 & \frac{1}{\bar{\rho}} \\ 0 & 0 & \bar{u}_x & 0 & 0 \\ 0 & 0 & \bar{u}_x & 0 & 0 \\ 0 & 0 & \bar{u}_x & 0 \\ 0 & 0 & \bar{u}_x \end{bmatrix}, \quad \boldsymbol{B} = \begin{bmatrix} \bar{u}_y & 0 & \bar{\rho} & 0 & 0 \\ 0 & \bar{u}_y & 0 & 0 & 0 \\ 0 & 0 & \bar{u}_y & 0 & \frac{1}{\bar{\rho}} \\ 0 & 0 & 0 & \bar{u}_y & 0 \\ 0 & 0 & \gamma \bar{p} & 0 & \bar{u}_y \end{bmatrix},$$

$$\boldsymbol{C} = \begin{bmatrix} \bar{u}_z & 0 & 0 & \bar{\rho} & 0 \\ 0 & \bar{u}_z & 0 & 0 & 0 \\ 0 & 0 & \bar{u}_z & 0 & 0 \\ 0 & 0 & 0 & \bar{u}_z & \frac{1}{\bar{\rho}} \\ 0 & 0 & 0 & \gamma \bar{p} & \bar{u}_z \end{bmatrix}, \quad \boldsymbol{D} = \begin{bmatrix} \nabla \cdot \bar{\boldsymbol{u}} & \frac{\partial \bar{\rho}}{\partial x} & \frac{\partial \bar{\rho}}{\partial y} & \frac{\partial \bar{\rho}}{\partial z} & 0 \\ 0 & \frac{\partial \bar{u}_x}{\partial x} & \frac{\partial \bar{u}_x}{\partial y} & \frac{\partial \bar{u}_x}{\partial z} & -\frac{1}{\gamma \bar{\rho} \bar{\rho}} \frac{\partial \bar{p}}{\partial z} \\ 0 & \frac{\partial \bar{u}_y}{\partial x} & \frac{\partial \bar{u}_y}{\partial y} & \frac{\partial \bar{u}_y}{\partial z} & -\frac{1}{\gamma \bar{\rho} \bar{\rho}} \frac{\partial \bar{p}}{\partial y} \\ 0 & \frac{\partial \bar{u}_z}{\partial x} & \frac{\partial \bar{u}_z}{\partial y} & \frac{\partial \bar{u}_z}{\partial z} & -\frac{1}{\gamma \bar{\rho} \bar{\rho}} \frac{\partial \bar{p}}{\partial z} \\ 0 & \frac{\partial \bar{p}}{\partial x} & \frac{\partial \bar{p}}{\partial y} & \frac{\partial \bar{p}}{\partial z} & \gamma (\nabla \cdot \bar{\boldsymbol{u}}) \end{bmatrix}$$

Here ρ is the density, u_x , u_y , u_z are the velocity components and p is the pressure. An over bar indicates the background mean flow and a prime indicates the small disturbances in the linearization.

For convenience of discussion, we denote (1) using a spatial operator L as

$$\frac{\partial \boldsymbol{w}}{\partial t} + \boldsymbol{L}(\boldsymbol{w}) = 0 \tag{2}$$

The Euler equation will also be referred to as the forward problem in this paper. The system of partial differential equations is supplemented with initial and boundary conditions.

Let the adjoint system for (1) be written as

$$\frac{\partial \tilde{\boldsymbol{w}}}{\partial t} + \tilde{\boldsymbol{A}} \frac{\partial \tilde{\boldsymbol{w}}}{\partial x} + \tilde{\boldsymbol{B}} \frac{\partial \tilde{\boldsymbol{w}}}{\partial y} + \tilde{\boldsymbol{C}} \frac{\partial \tilde{\boldsymbol{w}}}{\partial z} + \tilde{\boldsymbol{D}} \tilde{\boldsymbol{w}} = 0$$
 (3)

and denoted as

$$\frac{\partial \tilde{\boldsymbol{w}}}{\partial t} + \tilde{\boldsymbol{L}}(\tilde{\boldsymbol{w}}) = 0 \tag{4}$$

The variables associated with an adjoint system will be indicated by a tilde. The adjoint system is defined such that the following operation becomes valid:

$$\tilde{\boldsymbol{w}}^{T} \left[\frac{\partial \boldsymbol{w}}{\partial t} + \boldsymbol{L}(\boldsymbol{w}) \right] + \boldsymbol{w}^{T} \left[\frac{\partial \tilde{\boldsymbol{w}}}{\partial t} + \tilde{\boldsymbol{L}}(\tilde{\boldsymbol{w}}) \right] = \frac{\partial E}{\partial t} + \frac{\partial J_{x}}{\partial x} + \frac{\partial J_{y}}{\partial y} + \frac{\partial J_{z}}{\partial z} = \frac{\partial E}{\partial t} + \nabla \cdot \boldsymbol{J}$$
 (5)

where a superscript T denotes vector transpose, and $E(\boldsymbol{w}, \tilde{\boldsymbol{w}})$ and $J(\boldsymbol{w}, \tilde{\boldsymbol{w}}) = (J_x, J_y, J_z)$ are bi-linear functions of \boldsymbol{w} and $\tilde{\boldsymbol{w}}$. For (5) to be valid, it is straightforward to find that the adjoint system is obtained when

$$\tilde{A} = A^T, \ \tilde{B} = B^T, \ \tilde{C} = C^T, \ \tilde{D} = \frac{\partial A^T}{\partial x} + \frac{\partial B^T}{\partial y} + \frac{\partial C^T}{\partial z} - D^T$$
 (6)

with

$$E(\boldsymbol{w}, \tilde{\boldsymbol{w}}) = \tilde{\boldsymbol{w}}^T \boldsymbol{w} \tag{7}$$

and

$$J(\boldsymbol{w}, \tilde{\boldsymbol{w}}) = (\tilde{\boldsymbol{w}}^T A \boldsymbol{w}, \ \tilde{\boldsymbol{w}}^T B \boldsymbol{w}, \ \tilde{\boldsymbol{w}}^T C \boldsymbol{w})$$
(8)

It is also easy to find that the flux vector J is of the form

$$\boldsymbol{J} = (J_x, J_y, J_z) = (\tilde{\boldsymbol{w}}^T \cdot \boldsymbol{w}) \bar{\boldsymbol{u}} + (\bar{\rho}\tilde{\rho} + \gamma \bar{p}\tilde{p}) \boldsymbol{u}' + \frac{1}{\bar{\rho}} p' \tilde{\boldsymbol{u}}$$
(9)

It is to be noted that the adjoint system as defined in (3) is assumed to be non-zero for t < t' where t' is a bound for the time of interest in the Euler forward problem. As we will see later, the numerical solution

of the adjoint system may be computed in a time marching fashion in a reversed time variable $\tau = t' - t$, leading to

$$\frac{\partial \tilde{\boldsymbol{w}}}{\partial \tau} - \tilde{\boldsymbol{L}}(\tilde{\boldsymbol{w}}) = 0 \tag{10}$$

The adjoint system will also be referred to as the backward problem in the this paper.

II.B. Cylindrical Coordinates

The linearized Euler equations in cylindrical coordinates can be written as

$$\frac{\partial \mathbf{w}}{\partial t} + \mathbf{A} \frac{\partial \mathbf{w}}{\partial x} + \mathbf{B} \frac{\partial \mathbf{w}}{\partial r} + \frac{1}{r} \mathbf{C} \frac{\partial \mathbf{w}}{\partial \theta} + \frac{1}{r} \mathbf{D} \mathbf{w} + \mathbf{E} \mathbf{w} = 0$$
(11)

which we denote as

$$\frac{\partial \mathbf{w}}{\partial t} + \mathbf{L}_c(\mathbf{w}) = 0 \tag{12}$$

where

$$\boldsymbol{w} = \begin{bmatrix} \rho' \\ u'_x \\ u'_r \\ u'_\theta \\ p' \end{bmatrix}, \quad \boldsymbol{A} = \begin{bmatrix} \bar{u}_x & \bar{\rho} & 0 & 0 & 0 & 0 \\ 0 & \bar{u}_x & 0 & 0 & \frac{1}{\bar{\rho}} \\ 0 & 0 & \bar{u}_x & 0 & 0 \\ 0 & 0 & \bar{u}_x & 0 & 0 \\ 0 & \gamma \bar{p} & 0 & 0 & \bar{u}_x \end{bmatrix}, \quad \boldsymbol{B} = \begin{bmatrix} \bar{u}_r & 0 & \bar{\rho} & 0 & 0 \\ 0 & \bar{u}_r & 0 & 0 & 0 \\ 0 & 0 & \bar{u}_r & 0 & \frac{1}{\bar{\rho}} \\ 0 & 0 & 0 & \bar{u}_r & 0 \\ 0 & 0 & \gamma \bar{p} & 0 & \bar{u}_r \end{bmatrix},$$

$$C = \begin{bmatrix} \bar{u}_{\theta} & 0 & 0 & \bar{\rho} & 0 \\ 0 & \bar{u}_{\theta} & 0 & 0 & 0 \\ 0 & 0 & \bar{u}_{\theta} & 0 & 0 \\ 0 & 0 & 0 & \bar{u}_{\theta} & \frac{1}{\bar{\rho}} \\ 0 & 0 & 0 & \gamma \bar{p} & \bar{u}_{\theta} \end{bmatrix}, \quad D = \begin{bmatrix} \bar{u}_{r} + \frac{\partial \bar{u}_{\theta}}{\partial \theta} & 0 & \bar{\rho} & \frac{\partial \bar{\rho}}{\partial \theta} & 0 \\ 0 & 0 & 0 & \frac{\partial \bar{u}_{r}}{\partial \theta} & 0 \\ 0 & 0 & 0 & -2\bar{u}_{\theta} + \frac{\partial \bar{u}_{r}}{\partial \theta} & 0 \\ 0 & 0 & \bar{u}_{\theta} & \bar{u}_{r} & -\frac{1}{\gamma \bar{\rho} \bar{p}} \frac{\partial \bar{p}}{\partial \theta} \\ 0 & 0 & \gamma \bar{p} & \frac{\partial \bar{p}}{\partial \theta} & \gamma \bar{u}_{r} + \frac{\partial \bar{u}_{\theta}}{\partial \theta} \end{bmatrix}$$

$$\boldsymbol{E} = \begin{bmatrix} \frac{\partial \bar{u}_x}{\partial x} + \frac{\partial \bar{u}_r}{\partial r} & \frac{\partial \bar{p}}{\partial x} & \frac{\partial \bar{p}}{\partial r} & 0 & 0\\ 0 & \frac{\partial \bar{u}_x}{\partial x} & \frac{\partial \bar{u}_x}{\partial r} & 0 & -\frac{1}{\gamma \bar{\rho} \bar{p}} \frac{\partial \bar{p}}{\partial x} \\ 0 & \frac{\partial \bar{u}_r}{\partial x} & \frac{\partial \bar{u}_r}{\partial r} & 0 & -\frac{1}{\gamma \bar{\rho} \bar{p}} \frac{\partial \bar{p}}{\partial r} \\ 0 & \frac{\partial \bar{u}_\theta}{\partial x} & \frac{\partial \bar{u}_\theta}{\partial r} & 0 & 0 \\ 0 & \frac{\partial \bar{p}}{\partial x} & \frac{\partial \bar{p}}{\partial r} & 0 & \gamma \left(\frac{\partial \bar{u}_x}{\partial x} + \frac{\partial \bar{u}_r}{\partial r} \right) \end{bmatrix}$$

Now let the adjoint system for (11) be written as

$$\frac{\partial \tilde{\boldsymbol{w}}}{\partial t} + \tilde{\boldsymbol{A}} \frac{\partial \tilde{\boldsymbol{w}}}{\partial x} + \tilde{\boldsymbol{B}} \frac{\partial \tilde{\boldsymbol{w}}}{\partial r} + \frac{1}{r} \tilde{\boldsymbol{C}} \frac{\partial \tilde{\boldsymbol{w}}}{\partial \theta} + \frac{1}{r} \tilde{\boldsymbol{D}} \tilde{\boldsymbol{w}} + \tilde{\boldsymbol{E}} \tilde{\boldsymbol{w}} = 0$$
(13)

and be denoted as

$$\frac{\partial \tilde{\boldsymbol{w}}}{\partial t} + \tilde{\boldsymbol{L}}_c(\tilde{\boldsymbol{w}}) = 0 \tag{14}$$

In the cylindrical coordinates, the adjoint system is determined such that the following is valid:

$$\tilde{\boldsymbol{w}}^{T} \left[\frac{\partial \boldsymbol{w}}{\partial t} + \boldsymbol{L}_{c}(\boldsymbol{w}) \right] + \boldsymbol{w}^{T} \left[\frac{\partial \tilde{\boldsymbol{w}}}{\partial t} + \tilde{\boldsymbol{L}}_{c}(\tilde{\boldsymbol{w}}) \right] = \frac{\partial E}{\partial t} + \frac{\partial J_{x}}{\partial x} + \frac{\partial J_{r}}{\partial r} + \frac{1}{r} \frac{\partial J_{\theta}}{\partial \theta} + \frac{J_{r}}{r} = \frac{\partial E}{\partial t} + \nabla \cdot \boldsymbol{J}$$
 (15)

This leads to

$$\tilde{\boldsymbol{A}} = \boldsymbol{A}^T, \ \tilde{\boldsymbol{B}} = \boldsymbol{B}^T, \ \tilde{\boldsymbol{C}} = \boldsymbol{C}^T, \ \tilde{\boldsymbol{D}} = \frac{\partial \boldsymbol{C}^T}{\partial \theta} + \boldsymbol{B}^T - \boldsymbol{D}^T, \ \tilde{\boldsymbol{E}} = \frac{\partial \boldsymbol{A}^T}{\partial x} + \frac{\partial \boldsymbol{B}^T}{\partial r} - \boldsymbol{E}^T$$
 (16)

with

$$E(\boldsymbol{w}, \tilde{\boldsymbol{w}}) = \tilde{\boldsymbol{w}}^T \boldsymbol{w} \tag{17}$$

and

$$J(\boldsymbol{w}, \tilde{\boldsymbol{w}}) = (J_x, J_r, J_\theta) = (\tilde{\boldsymbol{w}}^T \boldsymbol{A} \boldsymbol{w}, \ \tilde{\boldsymbol{w}}^T \boldsymbol{B} \boldsymbol{w}, \ \tilde{\boldsymbol{w}}^T \boldsymbol{C} \boldsymbol{w})$$
(18)

III. Eigenvalues and eigenfunctions of the adjoint system with a uniform mean flow

We first study the eigenvalues and eigenfunctions associated with the adjoint system and the dispersion relations of the linear waves when the mean flow is uniform. With a uniform mean flow, the adjoint system as given by (6) is considerably simplified. The complete adjoint equations are

$$\frac{\partial \tilde{\rho}}{\partial t} + \bar{u}_x \frac{\partial \tilde{\rho}}{\partial x} + \bar{u}_y \frac{\partial \tilde{\rho}}{\partial y} + \bar{u}_z \frac{\partial \tilde{\rho}}{\partial z} = 0$$
(19)

$$\frac{\partial \tilde{u}_x}{\partial t} + \bar{u}_x \frac{\partial \tilde{u}_x}{\partial x} + \bar{u}_y \frac{\partial \tilde{u}_x}{\partial y} + \bar{u}_z \frac{\partial \tilde{u}_x}{\partial z} + \bar{\rho} \frac{\partial \tilde{\rho}}{\partial x} + \gamma \bar{p} \frac{\partial \tilde{p}}{\partial x} = 0$$
 (20)

$$\frac{\partial \tilde{u}_y}{\partial t} + \bar{u}_x \frac{\partial \tilde{u}_y}{\partial x} + \bar{u}_y \frac{\partial \tilde{u}_y}{\partial y} + \bar{u}_z \frac{\partial \tilde{u}_y}{\partial z} + \bar{\rho} \frac{\partial \tilde{\rho}}{\partial y} + \gamma \bar{p} \frac{\partial \tilde{\rho}}{\partial y} = 0$$
 (21)

$$\frac{\partial \tilde{u}_z}{\partial t} + \bar{u}_x \frac{\partial \tilde{u}_z}{\partial x} + \bar{u}_y \frac{\partial \tilde{u}_z}{\partial y} + \bar{u}_z \frac{\partial \tilde{u}_z}{\partial z} + \bar{\rho} \frac{\partial \tilde{\rho}}{\partial z} + \gamma \bar{p} \frac{\partial \tilde{\rho}}{\partial z} = 0$$
 (22)

$$\frac{\partial \tilde{p}}{\partial t} + \bar{u}_x \frac{\partial \tilde{p}}{\partial x} + \bar{u}_y \frac{\partial \tilde{p}}{\partial y} + \bar{u}_z \frac{\partial \tilde{p}}{\partial z} + \frac{1}{\bar{\rho}} \left(\frac{\partial \tilde{u}_x}{\partial x} + \frac{\partial \tilde{u}_y}{\partial y} + \frac{\partial \tilde{u}_z}{\partial z} \right) = 0$$
 (23)

While this system is not exactly the same as the linearized Euler equations, the solutions of the two formulations can be closely related. If we let

$$\tilde{\rho}' = \bar{\rho}\tilde{p} + \tilde{\rho}, \ \tilde{u}_x' = \frac{1}{\bar{\rho}}\tilde{u}_x, \ \tilde{u}_y' = \frac{1}{\bar{\rho}}\tilde{u}_y, \ \tilde{u}_z' = \frac{1}{\bar{\rho}}\tilde{u}_z, \ \tilde{p}' = \gamma\bar{p}\tilde{p} + \bar{\rho}\tilde{\rho}$$
 (24)

then, it is easy to see that $\tilde{\rho}'$, \tilde{u}_x' , \tilde{u}_y' , \tilde{u}_z' and \tilde{p}' will satisfy the Euler equations. In particular, there is a simple relation for the acoustic solutions. If u_a, v_a, w_a and p_a represent an acoustic solution of the Euler system, then the corresponding adjoint solution is given by

$$(\tilde{\rho}, \tilde{u}_x, \tilde{u}_y, \tilde{u}_z, \tilde{p}) = (0, \bar{\rho}u_a, \bar{\rho}v_a, \bar{\rho}w_a, \frac{1}{\gamma\bar{p}}p_a)$$
(25)

This solution will be referred to as the *adjoint acoustic wave*. Substitution of this solution into (5) yields an acoustic energy equation in a uniform mean flow. Furthermore, for the adjoint acoustic waves, with $\tilde{\rho} = 0$, the equations for \tilde{p} by (19)-(23) is

$$\left(\frac{\partial}{\partial t} + \bar{u}_x \frac{\partial}{\partial x} + \bar{u}_y \frac{\partial}{\partial y} + \bar{u}_z \frac{\partial}{\partial z}\right)^2 \tilde{p} - \bar{a}^2 \left(\frac{\partial^2 \tilde{p}}{\partial x^2} + \frac{\partial^2 \tilde{p}}{\partial y^2} + \frac{\partial^2 \tilde{p}}{\partial z^2}\right) = 0$$
(26)

where

$$\bar{a}^2 = \frac{\gamma \bar{p}}{\bar{\rho}}$$

Equation (26) is the usual acoustic wave equation with a uniform mean flow. This implies that the dispersion relations for linear acoustic waves of the adjoint system in a uniform mean flow will be identical to that of the Euler equations under similar boundary conditions.

IV. Orthogonality of eigenfunctions

In this section, we show that the eigenfunctions of the Euler and adjoint systems are orthogonal. This orthogonality will be useful in deriving the reciprocal relations in the next section. Start with the Lagrange identity, obtained by (5), namely,

$$\frac{\partial E(\boldsymbol{w}, \tilde{\boldsymbol{w}})}{\partial t} + \nabla \cdot \boldsymbol{J}(\boldsymbol{w}, \tilde{\boldsymbol{w}}) = 0$$
(27)

where $E(\boldsymbol{w}, \tilde{\boldsymbol{w}})$ and $J(\boldsymbol{w}, \tilde{\boldsymbol{w}})$ are given in (7)-(8) or (17)-(18) and consider a region with uniform mean flow and constant cross section D as shown in Figure 1. Integrate (27) over a volume $V = [x, x + \Delta] \times D$ formed between two cross sections at x and $x + \Delta$,

$$\frac{\partial}{\partial t} \int_{V} E(\boldsymbol{w}, \tilde{\boldsymbol{w}}) dV + \int_{V} \nabla \cdot \boldsymbol{J}(\boldsymbol{w}, \tilde{\boldsymbol{w}}) dV = 0$$

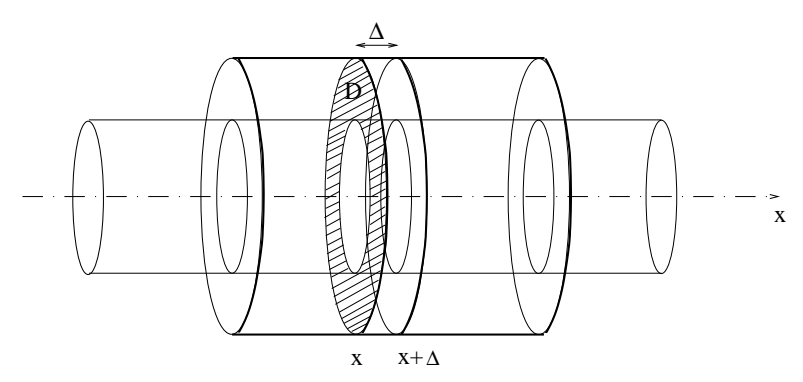


Figure 1. A duct with uniform cross section.

By divergence theorem, the above becomes

$$\frac{\partial}{\partial t} \int_{V} E(\boldsymbol{w}, \tilde{\boldsymbol{w}}) dV + \int_{\partial V} \boldsymbol{J}(\boldsymbol{w}, \tilde{\boldsymbol{w}}) \cdot \boldsymbol{n} dS = 0$$

where ∂V is the surface enclosing V and n is the normal vector outward from V. Since the boundary of V consists of the cross sections at x and $x + \Delta$ and duct side wall S, we have

$$\frac{\partial}{\partial t} \int_{V} E(\boldsymbol{w}, \tilde{\boldsymbol{w}}) dV + \int_{S} \boldsymbol{J}(\boldsymbol{w}, \tilde{\boldsymbol{w}}) \cdot \boldsymbol{n} dS - \int_{D_{x}} J_{x}(\boldsymbol{w}, \tilde{\boldsymbol{w}}) dS + \int_{D_{x+\Delta}} J_{x}(\boldsymbol{w}, \tilde{\boldsymbol{w}}) dS = 0$$

where J_x is the x-component of the J vector given in (8) and (18), and D_x and $D_{x+\Delta}$ denote the cross sections located at x and $x + \Delta$ respectively.

If we have, on duct side walls, that

$$\int_{S} J(\boldsymbol{w}, \tilde{\boldsymbol{w}}) \cdot \boldsymbol{n} dS = 0 \tag{28}$$

which is true on solid walls according to the normal flux expression given in (9), then,

$$\frac{\partial}{\partial t} \int_{V} E(\boldsymbol{w}, \tilde{\boldsymbol{w}}) dV - \int_{D_{x}} J_{x}(\boldsymbol{w}, \tilde{\boldsymbol{w}}) dS + \int_{D_{x+\Delta}} J_{x}(\boldsymbol{w}, \tilde{\boldsymbol{w}}) dS = 0$$
(29)

By a limit of $\Delta \to 0$, we get a conservation statement

$$\frac{\partial}{\partial t} \left[\int_{D} E(\boldsymbol{w}, \tilde{\boldsymbol{w}}) dS \right] + \frac{\partial}{\partial x} \left[\int_{D} J_{x}(\boldsymbol{w}, \tilde{\boldsymbol{w}}) dS \right] = 0$$
(30)

Now consider eigenfunctions of the Euler equations and adjoint system of the form

$$\mathbf{w}(x, y, z, t) = \mathbf{\phi}(k, y, z, \omega)e^{ikx - i\omega t}$$
(31)

$$\tilde{\boldsymbol{w}}(x,y,z,t) = \tilde{\boldsymbol{\phi}}(\tilde{k},y,z,\tilde{\omega})e^{i\tilde{k}x-i\tilde{\omega}t} \tag{32}$$

in which ω is the frequency and k is the wave number in x direction, where a dispersion relation of $k = k(\omega)$ is assumed. $\phi(k, r, \theta, \omega)$ and $\tilde{\phi}(\tilde{k}, r, \theta, \tilde{\omega})$ are the mode shape functions. Both of the above, as well as their complex conjugates satisfy the homogeneous system of equations (1) and (3). Substituting \boldsymbol{w} and $\tilde{\boldsymbol{w}}^*$ given by (31) and (32) into (30), we get

$$\frac{\partial}{\partial t} \int_{D} E(\phi, \ \tilde{\phi}^{*}) e^{i(k-\tilde{k}^{*})x-i(\omega-\tilde{\omega}^{*})t} dS + \frac{\partial}{\partial x} \int_{D} J_{x}(\phi, \ \tilde{\phi}^{*}) e^{i(k-\tilde{k}^{*})x-i(\omega-\tilde{\omega}^{*})t} dS = 0$$

which is

$$-i(\omega - \tilde{\omega}^*) \int_D E(\phi, \ \tilde{\phi}^*) dS + i(k - \tilde{k}^*) \int_D J_x(\phi, \ \tilde{\phi}^*) dS = 0$$
(33)

If we choose $\tilde{\omega} = \omega = \text{real}$, then the above is

$$\left[k(\omega) - \tilde{k}^*(\omega)\right] \int_D J_x(\phi, \ \tilde{\phi}^*) dS = 0$$

It follows that

$$\int_{D} J_{x}(\phi, \ \tilde{\phi}^{*})dS = 0, \ \text{if } k(\omega) \neq \tilde{k}^{*}(\omega)$$
(34)

To express this condition using the expression for J_x given in (8), we have

$$\int_{D} \tilde{\boldsymbol{\phi}}^{*T} \boldsymbol{A} \boldsymbol{\phi} dS = 0, \text{ if } k(\omega) \neq \tilde{k}^{*}(\omega)$$
(35)

That is, the eigenfunctions (mode shapes) of the Euler and adjoint systems corresponding to different eigenvalues are orthogonal in the sense of (34).

The orthogonality condition given explicitly is

$$\int_{D} \tilde{\boldsymbol{\phi}}^{*T} \boldsymbol{A} \boldsymbol{\phi} dS = \int_{D} \left[\bar{u}_{x} \left(\tilde{\phi}_{u}^{*} \phi_{u} + \tilde{\phi}_{v}^{*} \phi_{v} + \tilde{\phi}_{w}^{*} \phi_{w} + \tilde{\phi}_{p}^{*} \phi_{p} \right) + \gamma \bar{p} \tilde{\phi}_{p}^{*} \phi_{u} + \frac{1}{\bar{\rho}} \tilde{\phi}_{u}^{*} \phi_{p} \right] dS = 0, \text{ if } k(\omega) \neq \tilde{k}^{*}(\omega)$$
(36)

where the subscript in ϕ indicates the corresponding components of the eigenfunction ϕ and $\tilde{\phi}$.

V. Reciprocity

In this section, we derive two reciprocal relations between the solutions of the Euler and adjoint systems.

V.A. Reciprocity between a point source and duct modes

Consider the Greens function of the adjoint system defined by

$$\frac{\partial \tilde{\boldsymbol{w}}}{\partial t} + \tilde{\boldsymbol{L}}(\tilde{\boldsymbol{w}}) = -\delta(\boldsymbol{r} - \tilde{\boldsymbol{r}}')\delta(t - t')\boldsymbol{e}_{p}$$
(37)

with initial condition

$$\tilde{\boldsymbol{w}} = 0, \ t > t'$$

In the above, $e_p = (0, 0, 0, 0, 1)$. It is chosen for the convenience of establishing the reciprocal relations in pressure. Other choices are possible of course.

We study the case where the solution to the Euler equations, a forward problem, will be the one formed by an incoming wave mode inside the duct as shown in Figure 3. Specifically, let the solutions inside the duct be written in the frequency domain as

$$\mathbf{w}(\mathbf{r},t) = \mathbf{f}(x,r,\theta,\omega)e^{-i\omega t}$$
(38)

$$\tilde{\boldsymbol{w}}(\boldsymbol{r},t) = \tilde{\boldsymbol{f}}(x,r,\theta,\omega)e^{-i\omega t}$$
(39)

where, with a local uniform duct assumption, we have

$$\mathbf{f}(x, r, \theta, \omega) = A_{m_o n_o} \phi_{m_o n_o}(r, \theta) e^{ik_{m_o n_o}^+(\omega)x} + \sum_{m', n'} R_{m', n'} \phi_{m'n'}(r, \theta) e^{ik_{m'n'}^-(\omega)x}$$
(40)

$$\tilde{\mathbf{f}}(x,r,\theta,\omega) = \sum_{m,n} \tilde{A}_{mn} \tilde{\boldsymbol{\phi}}_{mn}(r,\theta) e^{ik_{mn}^{+}(\omega)x}$$
(41)

in which we have used the fact that eigenvalues of the adjoint system and the Euler equations are identical. Mode (m_o, n_o) is the incoming wave with amplitude $A_{m_o n_o}$, and $R_{m'n'}$ are the reflected wave amplitude of modes (m', n'). The solution to the adjoint system inside the duct is also decomposed into duct modes

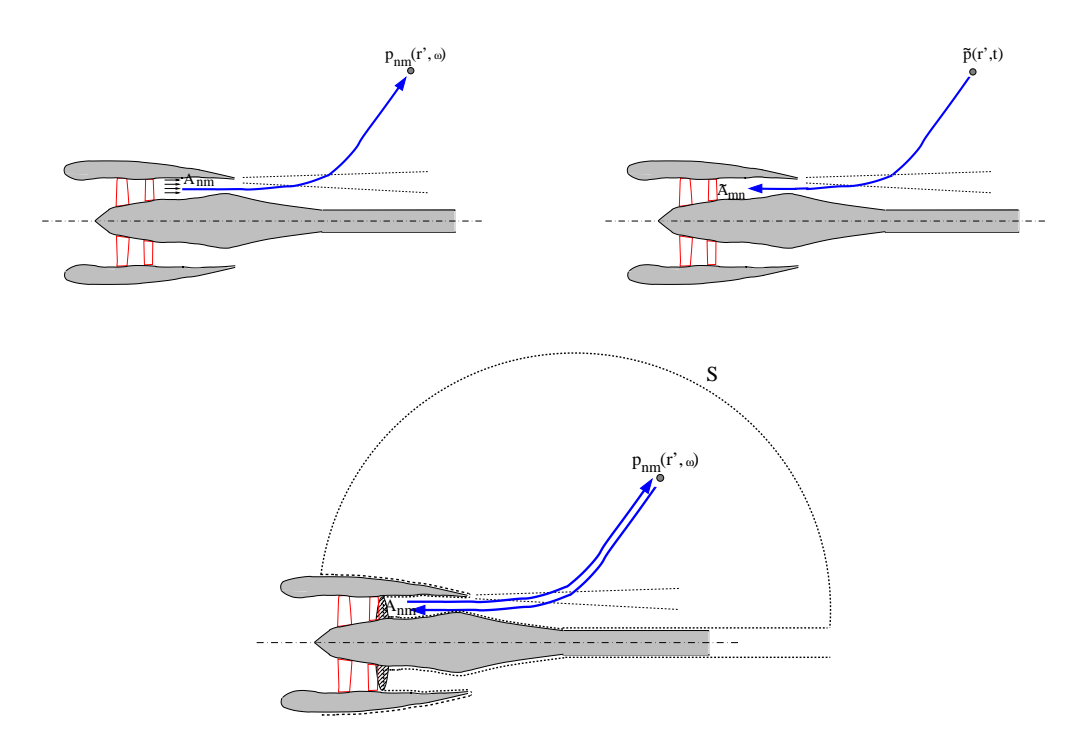


Figure 2. Schematic diagrams showing the forward and adjoint problems.

(m,n) with amplitudes denoted by \tilde{A}_{mn} . Since it is generated by a point source at the far field, the adjoint solution inside the duct near the inlet region should consist of only left traveling modes. By the results in section 2, these left traveling waves, when solved in the reversed time τ , have the same dispersion relations as the right traveling acoustic waves, as indicated by $k_{mn}^+(\omega)$ in (41).

In the frequency domain, we have

$$-i\omega \mathbf{f} + \mathbf{L}(\mathbf{f}) = 0 \tag{42}$$

and

$$-i\omega\tilde{\mathbf{f}} + \tilde{\mathbf{L}}(\tilde{\mathbf{f}}) = -\delta(\mathbf{r} - \tilde{\mathbf{r}}')\mathbf{e}_p \tag{43}$$

By an operation $\tilde{\boldsymbol{f}}^{*T}(42) + \boldsymbol{f}^T(43)^*$, we get

$$oldsymbol{ ilde{f}}^{*T}oldsymbol{L}(oldsymbol{u}) + oldsymbol{f}^T ilde{oldsymbol{L}}(ilde{oldsymbol{f}}^*) = -\delta(oldsymbol{r} - ilde{oldsymbol{r}}')oldsymbol{f}^T oldsymbol{e}_{n}$$

where a star indicates complex conjugate. Using the properties of the adjoint system discussed in the previous sections, the left hand side becomes a complete divergence and by the integration over a volume V in space, outlined in Figure 3, we get

$$\int_{V} \nabla \cdot \boldsymbol{J}(\boldsymbol{f}, \ \tilde{\boldsymbol{f}}^{*}) d\boldsymbol{r} = -p(\tilde{\boldsymbol{r}}', \omega)$$

Using again the divergence theorem and by letting the boundary of V in open space to go to infinite and applying the wall boundary conditions, we have

$$-\int_{D} J_{x}(\boldsymbol{f}, \ \tilde{\boldsymbol{f}}^{*})dS = -p(\tilde{\boldsymbol{r}}', \omega)$$

where D is area of cross section at the duct inlet region and J_x is the x component of the flux vector J in the Lagrange identity.

By substituting (40) and (41) into the above, due to orthogonality condition for the eigenfunctions (35), we get

$$\tilde{A}_{m_o n_o}^* A_{m_o n_o} \int_D \tilde{\boldsymbol{\phi}}^*_{m_o n_o}^T \boldsymbol{A} \boldsymbol{\phi}_{m_o n_o} dS = p(\tilde{\boldsymbol{r}}', \omega)$$
(44)

In other words, the adjoint solution can act as a filter for the modal contributions at the far field as noted in [7].

Finally, (44) can be written as

$$\frac{p(\tilde{r}',\omega)}{A_{m_o n_o}} = \alpha_{m_o n_o} \tilde{A}_{m_o n_o} \tag{45}$$

where the proportional constant

$$\alpha_{mn} = \int_{D} \tilde{\boldsymbol{\phi}}^{*T}_{mn} \boldsymbol{A} \boldsymbol{\phi}_{mn} dS$$

Equation (45) is the reciprocal relation between the acoustic pressure $p(\tilde{r}, \omega)$ at \tilde{r}' produced by duct mode (n_o, m_o) and the amplitude $\tilde{A}_{n_o m_o}$ of that mode inside the duct due to a point source at \tilde{r}' of the adjoint system.

Furthermore, if the duct cross section is independent of θ , let the eigenfunctions of the duct modes be expressed as

$$\phi_{mn}(r,\theta) = \begin{bmatrix} \phi_{\rho} \\ \phi_{u} \\ \phi_{v} \\ \phi_{w} \\ \phi_{p} \end{bmatrix} = \begin{bmatrix} \Psi_{mn}(r) \\ \frac{k_{mn}}{\omega - \bar{u}_{x}k_{mn}} \Psi_{mn}(r) \\ -\frac{i}{\omega - \bar{u}_{x}k_{mn}} \Psi'_{mn}(r) \\ \frac{m}{\omega - \bar{u}_{x}k_{mn}} \frac{\Psi_{mn}(r)}{r} \\ \Psi_{mn}(r) \end{bmatrix} e^{im\theta}, \quad \tilde{\phi}_{mn}(r,\theta) = \begin{bmatrix} \tilde{\phi}_{\rho} \\ \tilde{\phi}_{u} \\ \tilde{\phi}_{v} \\ \tilde{\phi}_{w} \end{bmatrix} = \begin{bmatrix} 0 \\ \bar{\rho} \frac{k_{mn}}{\omega - \bar{u}_{x}k_{mn}} \Psi'_{mn}(r) \\ -\bar{\rho} \frac{i}{\omega - \bar{u}_{x}k_{mn}} \Psi'_{mn}(r) \\ \bar{\rho} \frac{m}{\omega - \bar{u}_{x}k_{mn}} \frac{\Psi'_{mn}(r)}{r} \\ \frac{1}{\gamma \bar{p}} \Psi_{mn}(r) \end{bmatrix} e^{im\theta}$$

$$(46)$$

where $\Psi_{mn}(r)$ is the pressure eigenfunction of mode (m,n). It is straightforward to verify, by using the expressions in (36), that we have the proportional constant α_{mn} in (45) as

$$\alpha_{mn} = \int_{D} \tilde{\boldsymbol{\phi}}^{*T}_{mn} \boldsymbol{A} \boldsymbol{\phi}_{mn} dS = 4\pi \left(\bar{u}_{x} + \frac{\gamma \bar{p}}{\bar{\rho}} \frac{k_{mn}}{\omega - \bar{u}_{x} k_{mn}} \right) \int_{h}^{R} \Psi_{mn}^{2}(r) r dr = 4\pi \left(\frac{d\omega}{dk} \right)_{mn} \int_{h}^{R} \Psi_{mn}^{2}(r) r dr$$
(47)

where h and R are the lower and upper limits of duct cross section in r and $\left(\frac{d\omega}{dk}\right)_{mn}$ is the group velocity of mode (m,n).

In general, according to (33), we also have

$$\alpha_{mn} = \int_{D} \tilde{\boldsymbol{\phi}}^{*T}_{mn} \boldsymbol{A} \boldsymbol{\phi}_{mn} dS = \frac{\partial \omega}{\partial k} \int_{D} \tilde{\boldsymbol{\phi}}^{*T}_{mn} \boldsymbol{\phi}_{mn} dS$$
 (48)

which is the same as (47).

V.B. Reciprocity between duct modes

Consider a non-uniform duct as shown in Figure 3, with a region of varying duct area between $x = X_1$ and $x = X_2$. Assume that an incoming duct mode is present at the left side of the duct. Due to the non-uniform duct body, the incident wave will be reflected as well as transmitted to the other side of the non-uniform region. The incoming mode will also be scattered into other modes. Let's assume the solution in the two uniform regions be as follows:

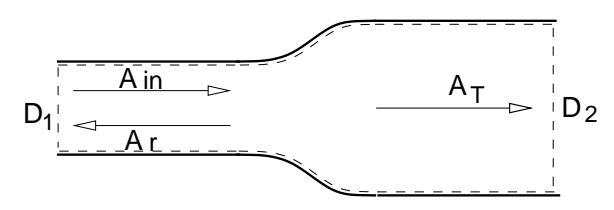
for $x < X_1$ (incoming and reflected waves):

$$\mathbf{f}(x, r, \theta, \omega) = A_{m_o n_o} \phi_{m_o n_o}(r, \theta) e^{ik_{m_o n_o}^+(\omega)x} + \sum_{m', n'} R_{m', n'} \phi_{m'n'}(r, \theta) e^{ik_{m'n'}^-(\omega)x}$$
(49)

for $x > X_2$ (transmitted waves):

$$f(x, r, \theta, \omega) = \sum_{m', n'} T_{m', n'} \phi_{m'n'}(r, \theta) e^{ik_{m'n'}^{\dagger}(\omega)x}$$
(50)

where $A_{n_0m_0}$ is the amplitude of the incoming mode, and $R_{n'm'}$ and $T_{n'm'}$ are the amplitudes of the reflected and transmitted wave modes respectively.



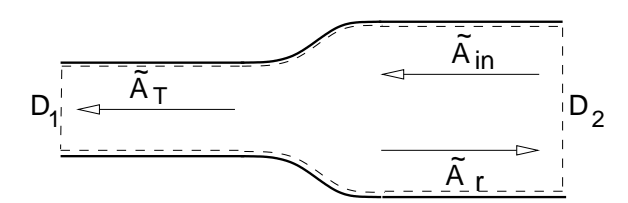


Figure 3. Schematic diagram showing a non-uniform duct and incident, reflected and transmitted waves.

For the adjoint problem, we consider an incoming wave mode at the other side and express the solution as follows:

for $x < X_1$ (transmitted waves):

$$\tilde{\mathbf{f}}(x, r, \theta, \omega) = \sum_{\tilde{m}', \tilde{n}'} \tilde{T}_{\tilde{m}', \tilde{n}'} \boldsymbol{\phi}_{\tilde{m}'\tilde{n}'}(r, \theta) e^{ik_{\tilde{m}'\tilde{n}'}^+(\omega)x}$$
(51)

for $x > X_2$ (incoming and reflected waves):

$$\tilde{\boldsymbol{f}}(\boldsymbol{x}, r, \theta, \omega) = \tilde{A}_{\tilde{m}_{o}\tilde{n}_{o}} \boldsymbol{\phi}_{\tilde{m}_{o}\tilde{n}_{o}}(r, \theta) e^{ik_{\tilde{m}_{o}\tilde{n}_{o}}^{+}(\omega)x} + \sum_{\tilde{m}', \tilde{n}'} \tilde{R}_{\tilde{m}', n'} \boldsymbol{\phi}_{\tilde{m}'\tilde{n}'}(r, \theta) e^{ik_{\tilde{m}'\tilde{n}'}^{-}(\omega)x}$$

$$(52)$$

By using the Lagrange identity (27) and an integral over a volume outlined in Figure 3, we have

$$\int_{D_1} J_x(\boldsymbol{f}, \tilde{\boldsymbol{f}}^*) dS - \int_{D_2} J_x(\boldsymbol{f}, \tilde{\boldsymbol{f}}^*) dS = 0$$

Then, by substituting (49)-(52) into the above, due to orthogonality of the eigenfunctions, we get

$$A_{n_o m_o} \tilde{T}_{m_o n_o} \int_{D_1} \tilde{\boldsymbol{\phi}}_{m_o n_o}^{*T} \boldsymbol{A} \boldsymbol{\phi}_{m_o n_o} dS = T_{\tilde{m}_o \tilde{n}_o} \tilde{A}_{\tilde{m}_o \tilde{n}_o} \int_{D_2} \tilde{\boldsymbol{\phi}}_{\tilde{m}_o \tilde{n}_o}^{*T} \boldsymbol{A} \boldsymbol{\phi}_{\tilde{m}_o \tilde{n}_o} dS$$
 (53)

Equation (53) is the reciprocal relation between duct modes of the Euler and adjoint systems. Using the proportional constant derived earlier, (53) can also be written more succinctly as

$$\alpha_{m_o n_o} \frac{\tilde{T}_{m_o n_o}}{\tilde{A}_{\tilde{m}_o \tilde{n}_o}} = \alpha_{\tilde{m}_o \tilde{n}_o} \frac{T_{\tilde{m}_o \tilde{n}_o}}{A_{m_o n_o}} \tag{54}$$

The above establishes the direct relationship between any transmitted mode $(\tilde{m}_o, \tilde{n}_o)$ due to the incident mode (m_o, n_o) of the Euler equations and those of the adjoint system due to an incident $(\tilde{m}_o, \tilde{n}_o)$ mode.

VI. Numerical solution of the adjoint system

VI.A. Time Domain Wave Packet method

In [13], a Time Domain Wave Packet (TDWP) method has been proposed for linear aeroacoustics computations. Some of its advantages have been mentioned in the introduction. A key element in TDWP is the modeling of the source term so that a wave packet is generated. Application of the TDWP method to the adjoint equations will be discussed in this section.

We first show an example of modeling the duct incoming waves in the TDWP method. To generate the duct modes, the pressure equation is modified with a source term as

$$\frac{\partial p}{\partial t} + \bar{u}_0 \frac{\partial p}{\partial x} + \gamma \bar{p}_0 \left(\frac{\partial u}{\partial x} + \frac{\partial u}{\partial y} + \frac{\partial u}{\partial z} \right) = \phi_{mn}(y, z) \Psi(t) e^{-\sigma(x - x_0)^2}$$
(55)

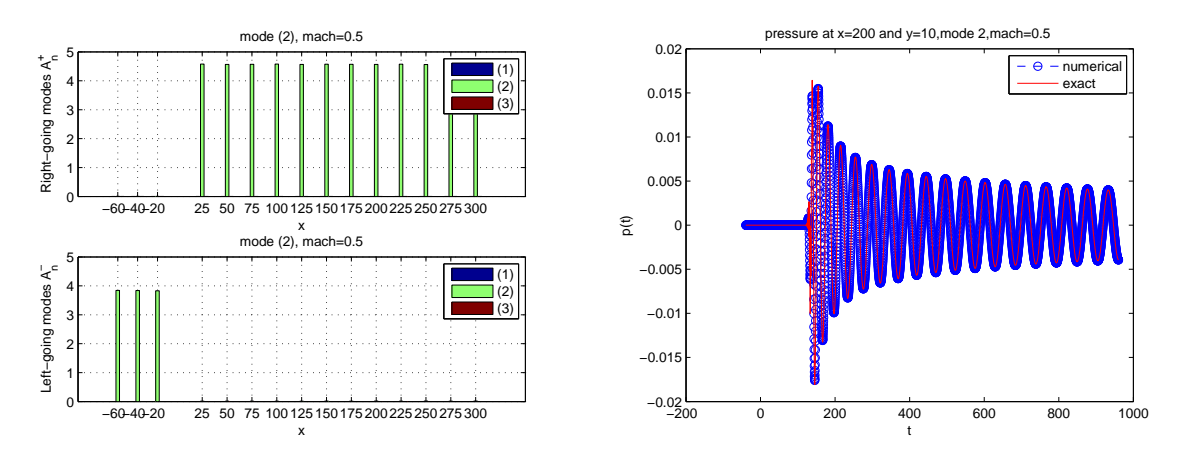


Figure 4. Left: Duct modes generated by the source term given in (55) in a uniform duct. (0,2) mode is introduced at $x_0 = 0$. Right: Time history of pressure at a fixed point and comparison with the exact solution.

where $\phi_{mn}(y,z)$ is the mode eigenfunction and $\Psi(t)$ is a broadband time pulse function that will be given later. The source term generates the specified wave mode of all the frequencies, as can be predicted by an analytic solution that will be shown elsewhere. In Figure 4, we show an example of two-dimension uniform duct with the forcing term applied. The source plane is placed at $x_0 = 0$ and the right and left going waves are generated correctly. A comparison in pressure history at a fixed point with the exact solution is also shown with good agreement.

VI.B. Initial condition for adjoint system

For reciprocal condition (45), a point source is placed at the far-field and we solve

$$\frac{\partial \tilde{\boldsymbol{u}}}{\partial t} + \tilde{\boldsymbol{L}}_c(\tilde{\boldsymbol{u}}) = -\Psi(t - t')\delta(\boldsymbol{r} - \tilde{\boldsymbol{r}}')\boldsymbol{e}_p \tag{56}$$

where \tilde{r}' is a far field observation point, t' is a time of interest, and $\Psi(t)$ is the broadband time function used in the Time Domain Wave Packet (TDWP) method. Function $\Psi(t)$ is non-zero for a finite time duration -T < t < T.

The time function $\Psi(t)$ used in this computation is as follows:¹³

$$\Psi(t) = \frac{\Delta t \sin(\omega_0 t)}{\pi t} e^{(\ln 0.01)(t/M\Delta t)^2}, \quad |t| \le M\Delta t$$

where $\omega_0 \Delta t = \pi/5$, M = 50.

Note that the time domain for which the solution of the adjoint system is nonzero is $t < t' + M\Delta t$. To solve (56) numerically in a time marching fashion, we introduce τ as

$$\tau = t' - t \tag{57}$$

This leads to the equation for numerical solution as

$$\frac{\partial \tilde{\boldsymbol{u}}}{\partial \tau} - \tilde{\boldsymbol{L}}_c(\tilde{\boldsymbol{u}}) = \Psi(-\tau)\delta(\boldsymbol{r} - \tilde{\boldsymbol{r}}')\boldsymbol{e}_p$$
 (58)

To deal with the delta function in the source term in (56), we use the exact acoustic solution in a uniform stream and recast (56) as an initial value problem. The details are described below.

At the far-field where the mean flow is assumed to be uniform, the exact solution to (58) can be found as the adjoint acoustic waves. Let

$$\tilde{P}^{(e)}(\boldsymbol{r},\tau) = \frac{\Psi(-\tau + \beta(x - \tilde{x}') + \bar{R}(\boldsymbol{r},\tilde{\boldsymbol{r}}')/c\alpha)}{4\pi c\alpha \bar{R}(\boldsymbol{r},\tilde{\boldsymbol{r}}')}$$

where

$$\alpha = \sqrt{1 - \bar{u}_x^2/c^2} = \sqrt{1 - M_x^2}, \quad \beta = \frac{\bar{u}_x}{c^2 - \bar{u}_x^2} = \frac{M_x}{c\alpha^2}, \quad \bar{R}(\boldsymbol{r}, \tilde{\boldsymbol{r}}') = \sqrt{(x - \tilde{x}')^2/\alpha^2 + (y - \tilde{y}')^2 + (z - \tilde{z}')^2}$$

Then, the exact solution $\tilde{\boldsymbol{w}}^{(e)}(\boldsymbol{r},\tau)$ to (58) for the density, pressure and velocity components of the adjoint solution is

$$\tilde{\rho}^{(e)}(x,r,\theta,\tau) = 0, \ \tilde{p}^{(e)}(x,r,\theta,\tau) = \left[\frac{\partial}{\partial \tau} - \bar{u}_x \frac{\partial}{\partial x}\right] \tilde{P}^{(e)}(r,\tau), \tag{59}$$

$$\tilde{u}_{x}^{(e)}(x,r,\theta,\tau) = \gamma \bar{p} \frac{\partial \tilde{P}^{(e)}}{\partial x}, \ \tilde{u}_{y}^{(e)}(x,r,\theta,\tau) = \gamma \bar{p} \frac{\partial \tilde{P}^{(e)}}{\partial u}, \ \tilde{u}_{z}^{(e)}(x,r,\theta,\tau) = \gamma \bar{p} \frac{\partial \tilde{P}^{(e)}}{\partial z}$$
(60)

and

$$\tilde{u}_r^{(e)}(x, r, \theta, \tau) = \tilde{u}_u^{(e)} \cos \theta + \tilde{u}_z^{(e)} \sin \theta, \quad \tilde{u}_{\theta}^{(e)}(x, r, \theta \tau) = -\tilde{u}_u^{(e)} \sin \theta + \tilde{u}_z^{(e)} \cos \theta \tag{61}$$

Since the source term in (58) becomes zero for $\tau > T$, equation (58) can be solved as an initial boundary value problem without the source term, with an initial condition as

$$\tilde{\boldsymbol{w}}(\boldsymbol{r},\tau)|_{\tau=\tau_0} = \tilde{\boldsymbol{w}}^{(e)}(\boldsymbol{r},\tau)\Big|_{\tau=\tau_0}$$
(62)

where τ_0 is any time greater than T.

Additionally, the exact solution given in (59)-(61) can also be utilized to recast (58) into a scattering problem with a homogeneous source term.

VI.C. Reduction in θ

The equations to be solved can be further reduced by decomposing the solution in the azimuthal angle θ when the geometry is independent of θ . In such cases,

$$\tilde{\boldsymbol{w}}(x,r,\theta,t) = \sum_{m=-L_m/2}^{L_m/2-1} \tilde{\boldsymbol{w}}_m(x,r,t)e^{im\theta}$$
(63)

where L_m is the number of terms kept in the expansion.

Then, the adjoint system (13) reduces to the following system in real variables,

$$\frac{\partial \hat{\boldsymbol{w}}_m}{\partial \tau} - \tilde{\boldsymbol{A}} \frac{\partial \hat{\boldsymbol{w}}_m}{\partial x} - \tilde{\boldsymbol{B}} \frac{\partial \hat{\boldsymbol{w}}_m}{\partial r} - \frac{m}{r} \hat{\boldsymbol{C}} \hat{\boldsymbol{w}}_m - \frac{1}{r} \tilde{\boldsymbol{D}} \hat{\boldsymbol{w}}_m - \tilde{\boldsymbol{E}} \hat{\boldsymbol{w}}_m = 0$$
 (64)

where

The initial condition for (64) is

$$\hat{\boldsymbol{w}}_m(x, r, \tau_0) = \hat{\boldsymbol{w}}_m^{(e)}(x, r, \tau_0)$$

where

$$\hat{\boldsymbol{w}}_{m}^{(e)}(x,r,\tau) = \frac{1}{2\pi} \int_{0}^{2\pi} \tilde{\boldsymbol{w}}^{(e)}(x,r,\theta,\tau) e^{-im\theta} d\theta$$
 (65)

For the given broadband function $\Psi(t)$, equation (65) may be evaluated numerically by FFT. The complete solution of the adjoint system can then be constructed using (63).

VII. Numerical results

In this section, we present numerical results of the adjoint system for the NASA/GE Fan Noise Source Diagnostic Test (SDT) exhaust radiation problem. In Figure 5, the computational domain is sketched. Two finite difference domains are used to cover (1) the region inside the duct starting at the vane trailing edges and (2) the exterior region that is extended to include the far field observation points. A time domain finite difference scheme is used. The spatial derivatives are approximated by a 7-point stencil as in the Dispersion Relation Preserving (DRP) scheme. Time integration is carried using the Low Dissipation

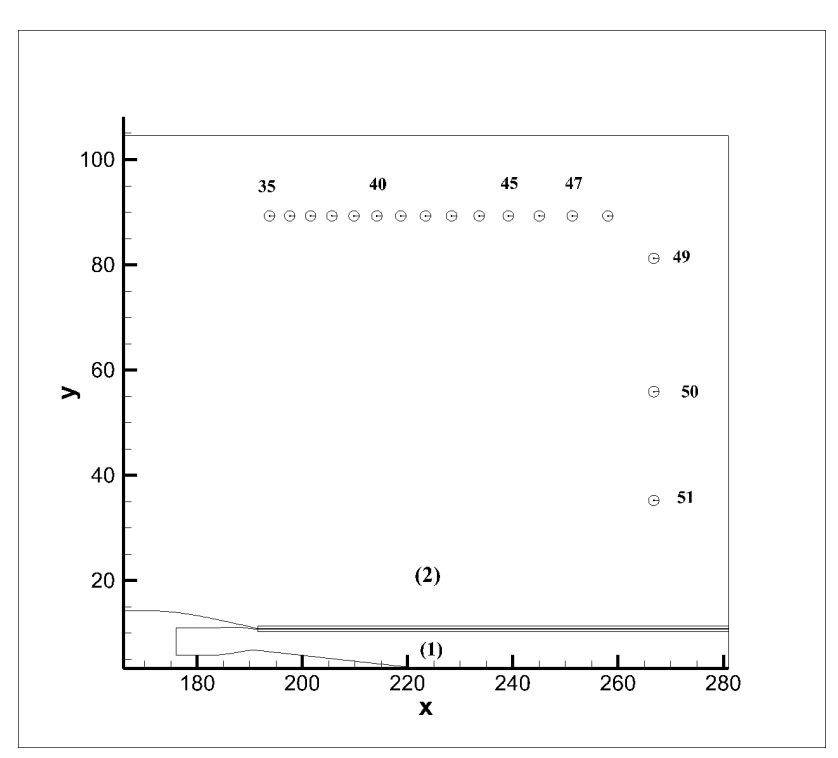


Figure 5. Computational domain for the adjoint system, showing the engine nacelle and far-field observation locations.

and Low Dispersion Runge-Kutta scheme (LDDRK 56).¹² Perfectly Matched Layer absorbing boundary condition is applied at all non-reflecting boundaries, including the one at the duct inlet.^{9–11} More details on the forward problem can be found in [13].

Computations are presented for an approach condition (61.7% of design speed) for the case of 22 blades and 54 vanes. At this condition, the Tyler-Sofrin interaction mode (m = -10) is by far the most dominant duct mode according to experimental modal studies.^{2,7,16,20} For this reason, the azimuthally reduced equation (64) is used in the computation. The initial condition in the computation is that given by (65). The broadband pulse generated by a point source for the adjoint system as a function of θ is shown in Figure 6 for the pressure component. Its decomposition in azimuthal modes is shown in Figure 7.

Computation starts at a non-dimensional time t = 8. In Figure 8, the numerical solution at a later time t = 11.5 is compared with the exact pulse solution given in (59)-(61). The external flow has a Mach number 0.1. The good agreement between the computed and theoretical solutions indicates that the initial state given in (62) has been implemented correctly.

A time sequence of pressure contours is shown in Figure 9. The time domain wave packet is reflected by the nacelle and the center-body, as well as propagated into the duct. The frequency domain solution, obtained by an FFT of the time domain solution shown in Figure 9, is plotted in Figure 10 at 2BPF. As noted earlier, the solution at other frequencies are also available in the same computation.

To compare with far field experimental results, and to demonstrate the reciprocal relations between the Euler and adjoint solutions, we show in Figure 11(top) the far field pressure amplitudes at the observation points corresponding to each propagating radial mode of the duct. The pressure amplitudes are plotted as a function of observation angle (geometric), measured from the forward axis. It shows the most effective radiation angle of each mode and the relative strengths of these modes when the incoming modal amplitude is unity. In Figure 11(bottom), we show the modal decomposition of the adjoint system where the far field source location is as indicated. The relative strengths of each radial mode are clearly similar to those predicted by the reciprocal condition (45). The comparison is very favorable. Although there are still some slight discrepancies in certain modal amplitudes, that may be due to the fact that, for simplicity of generating the mean flow, a one-dimensional mean flow has been used inside the duct which does not satisfy the wall

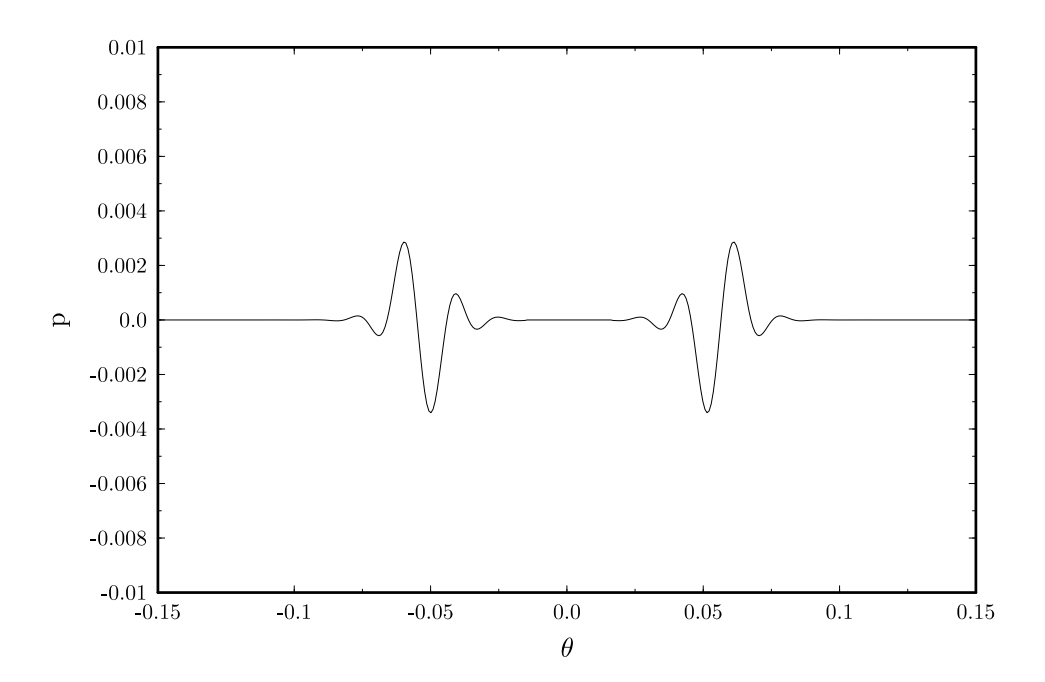


Figure 6. $\tilde{p}^{(e)}$ as a function of θ at a fixed (x,r) location close to the source.

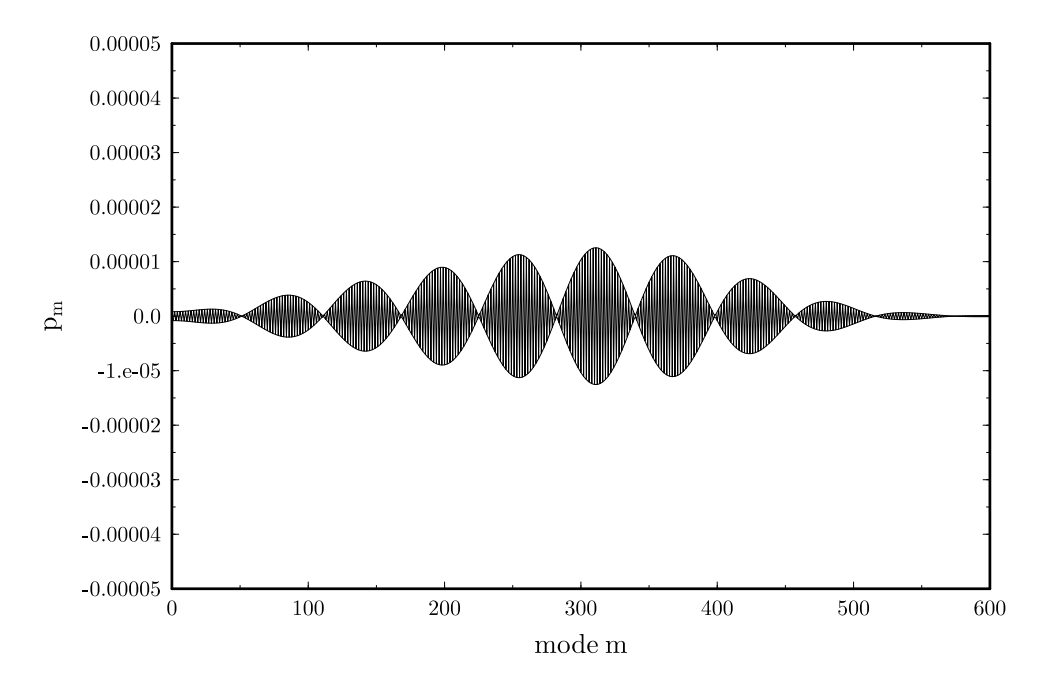


Figure 7. Modal decomposition of the exact solution shown in Figure 6 in azimuthal modes.

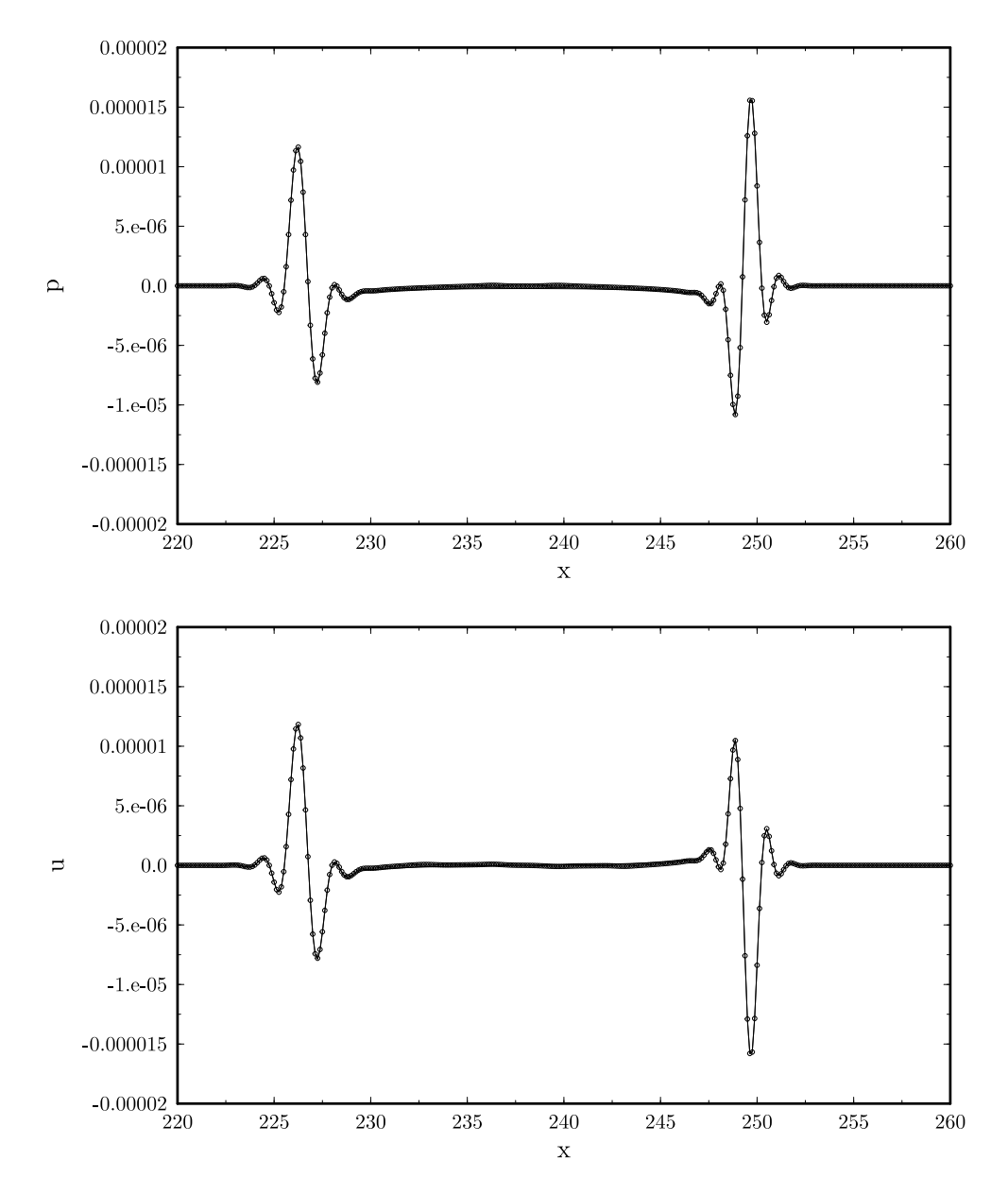


Figure 8. Pressure (top) and u-velocity (bottom) at time t=11.5 of the adjoint solution. Computation is started at t=8 with initial condition given by (59)-(61). Line: numerical; Symbol: exact solution.

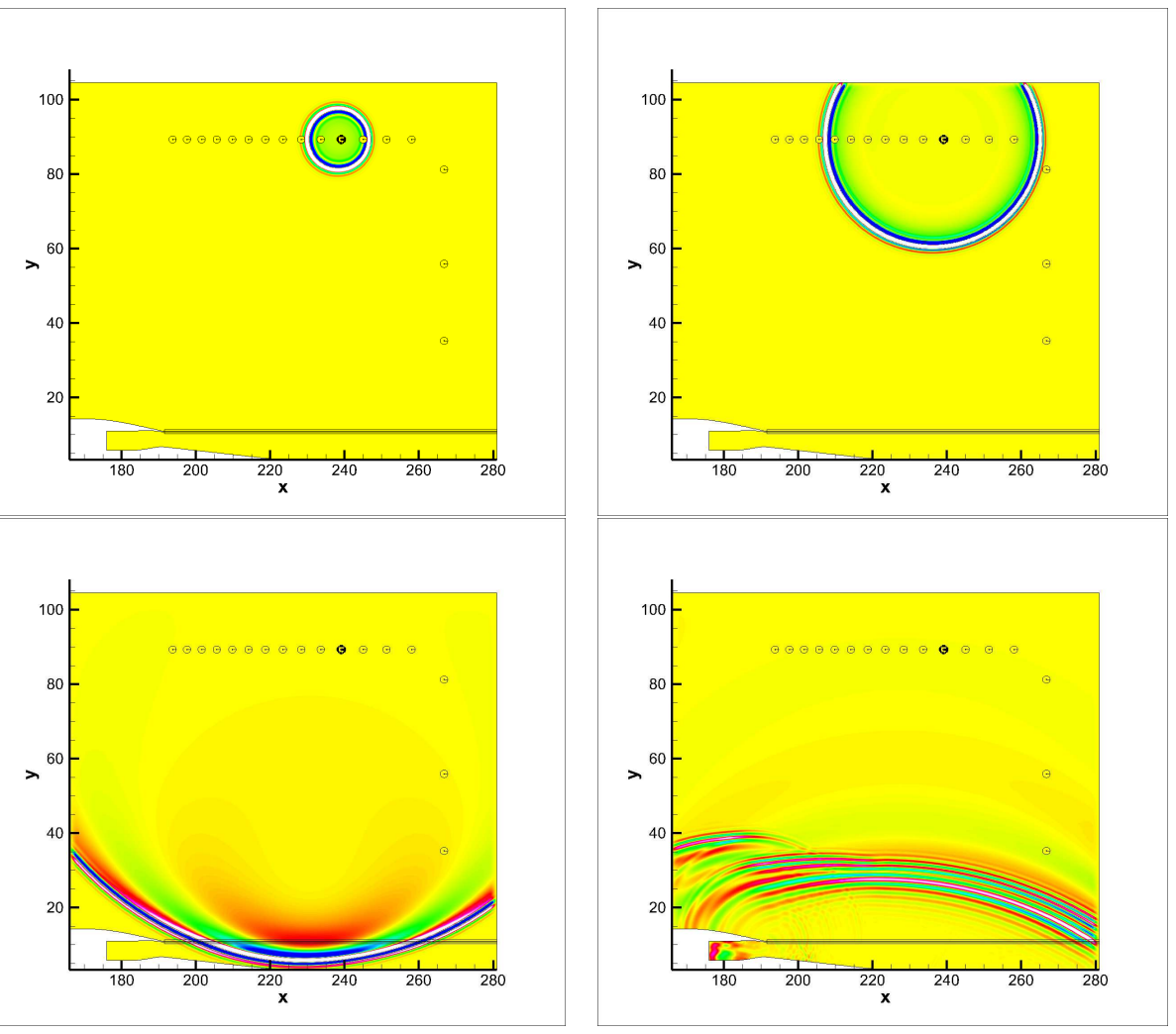


Figure 9. Contours of pressure at four chosen moments of the adjoint solution for a broadband point source placed at the indicated observation location.

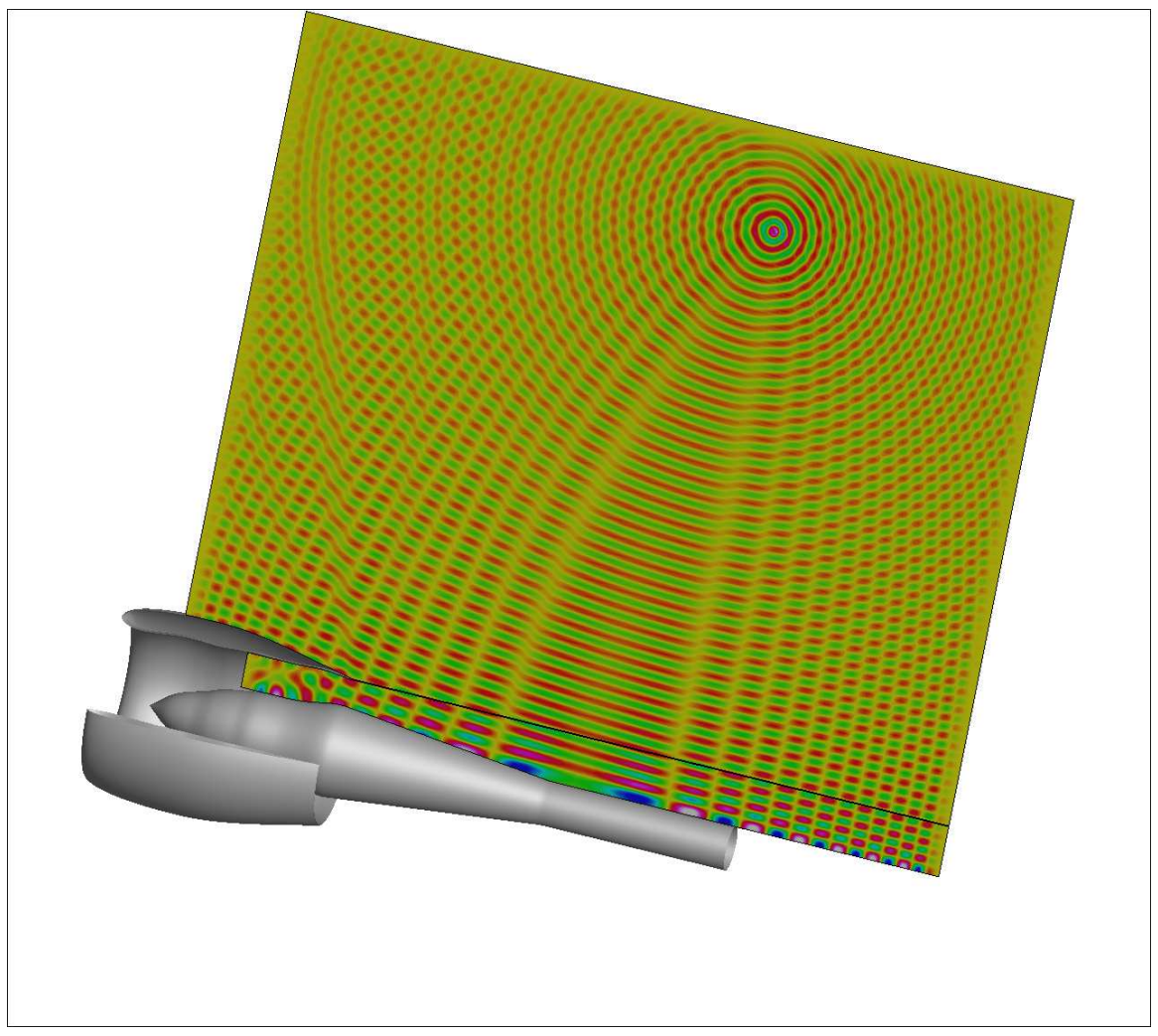
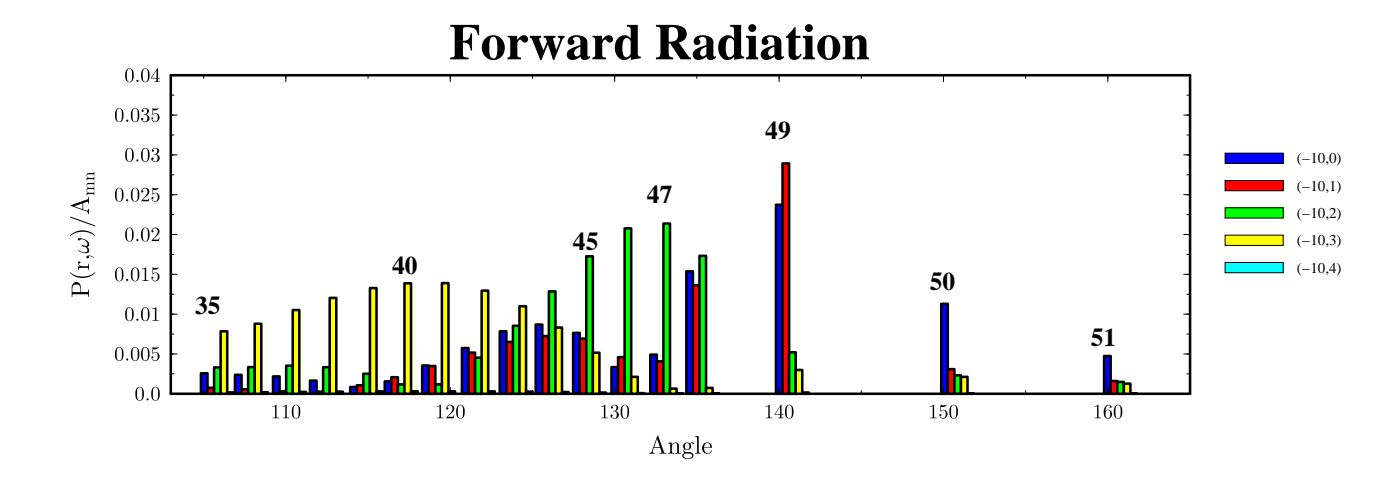


Figure 10. Frequency domain pressure contours at 2BPF by FFT of the time domain solution given in Figure 9.



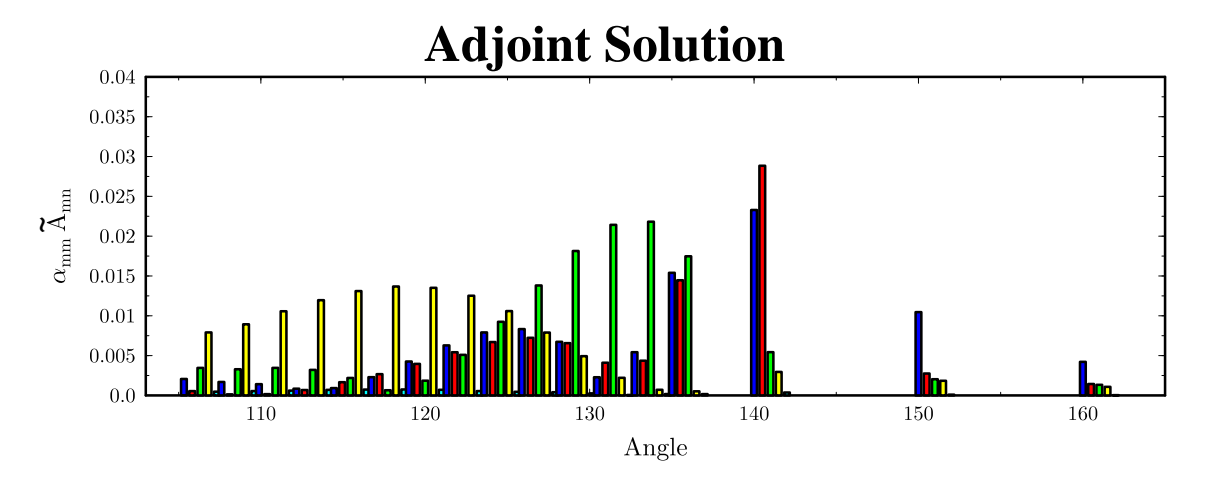


Figure 11. demonstration of reciprocity (45). Top: Far field pressure amplitude, $p(\tilde{r}', \omega)/A_{mn}$, produced by indicated duct mode normalized by the mode incoming amplitude. The duct input mode is indicated by the color and observation points as defined in Figure 5 are indicated by the numbers. Bottom: Modal amplitudes, $\alpha_{mn}\tilde{A}_{mn}$, of the adjoint problem when a point source is placed at the corresponding far field observation point.

boundary condition exactly. Further investigation will be presented in future work.

VIII. Conclusions

Adjoint systems for the linearized Euler equations in the Cartesian and Cylindrical coordinates have been studied in the time domain. A relation between the acoustics solutions of the Euler and adjoint equations in a uniform mean flow is given and it is further shown, under a local uniform flow assumption, that the linear waves in the two systems have the same dispersion relations and their the eigenfunctions are orthogonal in the sense of (36). A reciprocal relation between the in-duct propagating modes and the far-field pressure field has been derived in the presence of mean flow. A reciprocal relation for transmitted waves inside the duct is also derived. The reciprocity can be a useful tool in validating numerical solutions.

Furthermore, techniques for computing the adjoint Green's function by the Time Domain Wave Packet (TDWP) method are presented. Numerical results for the SDT aft radiation problem are shown where the reciprocal relation has been demonstrated. Good numerical accuracy has been observed in the validation of reciprocal relation derived in the paper.

Acknowledgment

This work is supported by the AeroAcoustics Research Consortium (AARC). This work used the Extreme Science and Engineering Discovery Environment (XSEDE), which is supported by National Science Foundation grant number OCI-1053575. Partial support from SRFDP-2009110211001 and the 111 Project B07009 of China is also acknowledged (XDL). We thank Dr. Edmane Envia of NASA Glenn Research Center for providing SDT geometry and associated mean flow data to one of the author (FQH).

References

- ¹Y-C Cho, Reciprocity principle in duct acoustics, J. Acoust. Soc. Am, Vol. 67, No. 5, 1980
- ²E. Envia, D. L. Tweedt, R. P. Woodward, D. M. Elliott, E. B. Fite, C. E. Hughes, G. G. Podboy and D. L. Sutliff, An assessment of current fan noise prediction capability, NASA TM 2008-215415, 2008
- ³W. Everseman, A reciprocal relation for transmission in non-uniform hard walled ducts without flow, Journal of Sound and Vibration, Vol. 47, 515-521, 1976.
- ⁴O. A. Godin, Reciprocity and energy conservation within the parabolic approximation, Wave Motion, Vol. 29, 175-194, 1999.
- ⁵J. B. Freund, Adjoint-based optimization for understanding and suppressing jet noise, Journal of Sound and Vibration, Vol. 330, 4114-4122, 2011
- ⁶C. E. Grosch and H. Salwen, The continuous spectrum of the Orr-Sommerfeld equation. Part I. The spectrum and the eigenfunctions, Journal of Fluid Mech., Vol. 87, 33-54, 1978.
- ⁷L. J. Heidelberg, Fan Noise Source Diagnostic Test Tone modal structure results, NASA TM 2002-211594, 2002
- ⁸D. C. Hill, Adjoint systems and their role in the receptivity problem for boundary layers, J. Fluid Mech., Vol.292, 183-204, 1995
- ⁹F. Q. Hu, Absorbing boundary conditions, International Journal of Computational Fluid Dynamics, Vol. 18, 513-522, 2004.
- ¹⁰F. Q. Hu, A Perfectly Matched Layer absorbing boundary condition for linearized Euler equations with a non-uniform mean flow, Journal of Computational Physics, Vol. 208, 469-492, 2005
- ¹¹F. Q. Hu, X. D. Li and D.K. Lin, Absorbing boundary conditions for nonlinear Euler and Navier-Stokes equations based on the perfectly matched layer technique, Journal of Computational Physics, Vol. 227, 4398-4424, 2008
- ¹²F. Q. Hu, M. Y. Hussaini and J. L. Manthey, Low-dissipation and low-dispersion Runge-Kutta schemes for computational acoustics, Journal of Computational Physics, Vol. 124, 177-191, 1996.
- ¹³F. Q. Hu, X. D. Li, X. Y. Li and M. Jiang, Time Domain Wave Packet method and suppression of instability waves in aeroacoustic computations, AIAA paper 2011-2891, 2011
- ¹⁴W. Mohring, On energy, group velocity and small damping of sound waves in ducts with shear flow, Journal of Sound and Vibration, Vol. 29, 93-101, 1973.
- ¹⁵W. Mohring, Energy conservation, time-reversal invariance and reciprocity in ducts with flow, Journal of Fluid Mech., Vol. 431, 223-237, 2001.
- ¹⁶D. M. Nark, E. Envia and C. L. Burley, On acoustic source specification for rotor-stator interaction noise prediction, AIAA paper 2010-3713, 2010
- ¹⁷H. Salwen and C. E. Grosch, The continuous spectrum of the Orr-Sommerfeld equation. Part II, Eigenfunction expansions, Journal of Fluid Mech., Vol. 104, 445-465, 1981.

- 18 C. K. W. Tam and J. C. Webb, Dispersion relation preserving finite difference schemes for computational acoustics, Journal of Computational Physics, Vol. 107, 262-281, 1993.
- 19 C. K. W. Tam and L. Auriault, Mean flow refraction effects on sound radiated from localized sources in a jet, J. Fluid Mech., Vol. 370, 145-174, 1998
- $^{20}\mathrm{R.~P.~Woodward,~C.~E.~Hughes,~R.~J.~Jeracki and~C.~J.~Miller,~Fan~Noise~Source~Diagnostic~Test~-$ Far-field acoustic results, NASA TM 2002-211591, 2002.